

## Phonon anomalies in $\text{Pb}_{1-x}\text{La}_x(\text{Zr}_{0.9}\text{Ti}_{0.1})\text{O}_3$ ceramics

E. Buixaderas,<sup>1,a)</sup> I. Gregora,<sup>1</sup> S. Kamba,<sup>1</sup> P. Kužel,<sup>1</sup> and I. Reaney<sup>2</sup>

<sup>1</sup>*Institute of Physics, ASCR v.v.i., Na Slovance 2, 182 21 Prague 8, Czech Republic*

<sup>2</sup>*University of Sheffield, Mappin Street, Sheffield, S1 3JD, United Kingdom*

(Received 20 December 2008; accepted 8 January 2009; published online 3 February 2009)

The lattice dynamics of  $\text{Pb}_{1-x}\text{La}_x(\text{Zr}_{0.9}\text{Ti}_{0.1})\text{O}_3$  (PLZT X/90/10) with  $X=0, 2, 4, 10\%$  of La was studied by means of Far Infrared, Raman and terahertz spectroscopies in the temperature range of 20–800 K. Infrared active soft phonons with anomalies near the paraelectric-ferroelectric phase transition were found for all the samples. Some Raman active phonons show anomalies  $\sim 200$  K below  $T_C$ , due to another phase transition to a ferroelectric state with doubled unit cell. Samples with higher La content ( $X=4, 10$ ) display nonclassical phonon softening described by  $\omega^2=a(T-T_C)^\gamma$  with  $\gamma=2/3$ . © 2009 American Institute of Physics. [DOI: 10.1063/1.3077019]

Lanthanum modified lead zirconate titanate ceramics  $\text{Pb}_{1-x}\text{La}_x(\text{Zr}_y\text{Ti}_{1-y})\text{O}_3$  (PLZT X/Y/1-Y, where  $X=100x$ ,  $Y=100y$ ) have been very well known since the seventies because of their exceptional optical and dielectric properties.<sup>1</sup> However the relationship between the local structure and macroscopic properties has not yet been solved.

Lanthanum doping of  $\text{Pb}(\text{Zr}_y\text{Ti}_{1-y})\text{O}_3$  (PZT) induces phase transitions and sometimes relaxor properties. At room temperature, PZT is rhombohedral for  $Y=60-94$ , with doubled unit cell due to oxygen octahedra tilts.<sup>2,3</sup> PZT 90/10 is ferroelectric (FE) and rhombohedral<sup>4</sup> at room temperature, but neutron diffraction<sup>3</sup> revealed superstructure peaks, which were interpreted also as a sign of orthorhombic symmetry.<sup>5</sup> The macroscopic symmetry of PLZT X/90/10 is still controversial.

PZT with  $\sim 94\%$  of Zr exhibits a morphotropic phase boundary between FE rhombohedral and an antiferroelectric (AFE) orthorhombic phase.<sup>2</sup> The location and shape of the morphotropic phase boundary is very sensitive to the addition of La.<sup>6</sup> Symmetry and polar character of PLZT X/90/10 also change; for small amounts of La ( $X \leq 2$ ) the macroscopic symmetry remains rhombohedral, but for  $X \geq 4$  the tetragonal symmetry together with an incommensurate superstructure is developed.<sup>7</sup> The local symmetry, however, seems to be monoclinic.

Raman scattering of PZT 90/10 ceramics<sup>8</sup> and single crystals<sup>9</sup> revealed a soft mode of E(TO) symmetry with minimum frequency  $\sim 200$  K, below the para-FE phase transition temperature  $T_C$ , as well as a new mode near  $50 \text{ cm}^{-1}$ , both related probably with the doubling of the unit cell at 380 K. In PLZT 2/95/5 ceramics<sup>10</sup> and thin films,<sup>11</sup> an infrared (IR) active soft mode was found. Its frequency shows surprisingly no anomaly near  $T_C=470$  K but it continuously decreases on heating up to 680 K, reminding the Burns temperature in relaxor FEs.

In this letter we present experimental data on PLZT X/90/10 ceramics obtained by Raman, IR, and time-domain terahertz (TDTHz) spectroscopies in the temperature range 20–800 K. The aim of the work was to understand the nature of the phase transitions by investigation of the associated soft modes. Samples with  $X=0, 2, 4$ , and 10 were prepared by a conventional mixed oxide routine. Their characterization by

x-ray diffraction, transmission electron microscopy (TEM), and dielectric measurements was already published.<sup>7</sup> IR reflectivity and Raman scattering were measured on polished ceramic disks. The TDTHz transmission measurements were carried out on thin polished plane-parallel samples (of  $30 \mu\text{m}$  thickness). Details about the experiments can be found elsewhere.<sup>12,13</sup>

The IR reflectivity spectra of PLZT X/90/10 at several temperatures are shown in Fig. 1. The reflectivity data below  $30 \text{ cm}^{-1}$  were calculated from the TDTHz experiment. All the samples show almost identical spectra at high temperatures in the cubic paraelectric (PE) phase. However, in the low temperature phases, different spectral features are observed for different samples, confirming the symmetry change on adding lanthanum.

Especially interesting is the behavior of the modes developing from the lowest-frequency cubic triplet  $F_{1u}$ . At 20 K the two peaks near  $100 \text{ cm}^{-1}$  do not develop so strongly in the  $X=4, 10$  samples. The dip at  $280 \text{ cm}^{-1}$  is also less remarkable in the samples with higher La content.

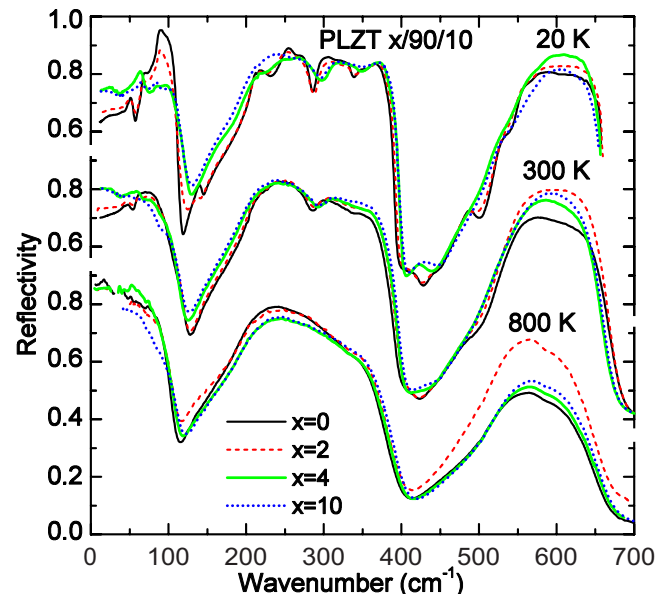


FIG. 1. (Color online) IR spectrum of the four PLZT X/90/10 ceramics at several temperatures.

<sup>a)</sup>Electronic mail: buixader@fzu.cz.

The IR reflectivity spectra were fitted together with the terahertz complex dielectric spectra  $\varepsilon^*(\omega) = \varepsilon'(\omega) - i\varepsilon''(\omega)$  using the factorized oscillator model,<sup>14</sup>

$$\varepsilon^*(\omega) = \varepsilon_\infty \prod_j \frac{\omega_{LOj}^2 - \omega^2 + i\omega\gamma_{LOj}}{\omega_{TOj}^2 - \omega^2 + i\omega\gamma_{TOj}}, \quad (1)$$

where  $\varepsilon_\infty$  is the permittivity at frequencies much higher than all polar phonon frequencies,  $\omega_{TOj}$  and  $\omega_{LOj}$  denote the transverse and longitudinal frequency of the  $j$ -th polar phonon, respectively, and  $\gamma_{TOj}$  and  $\gamma_{LOj}$  denote their corresponding damping constants. Then, the reflectivity  $R(\omega)$  is calculated by

$$R(\omega) = \left| \frac{\sqrt{\varepsilon^*(\omega)} - 1}{\sqrt{\varepsilon^*(\omega)} + 1} \right|^2. \quad (2)$$

In Table I we show the transition temperatures measured on cooling at 1 MHz for all the samples.  $T_{C'}$  refers to the transition to the second rhombohedral phase with doubled unit cell. More detailed dielectric data obtained at microwave and radio frequencies will be published elsewhere. In Fig. 2 the dielectric loss spectra  $\varepsilon''(\omega)$ , directly measured in the tera-

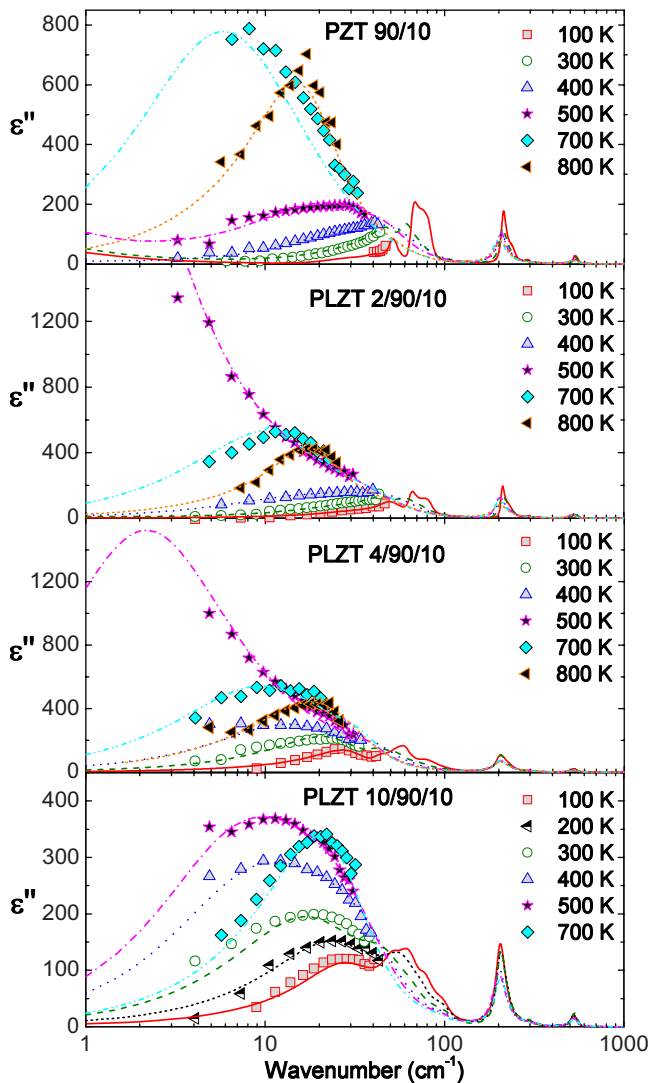


FIG. 2. (Color online) Imaginary part of permittivity  $\varepsilon''(\omega)$  for the PLZT samples at several temperatures. Symbols correspond to the terahertz experiment, lines to the spectral fits [Eqs. (1) and (2)].

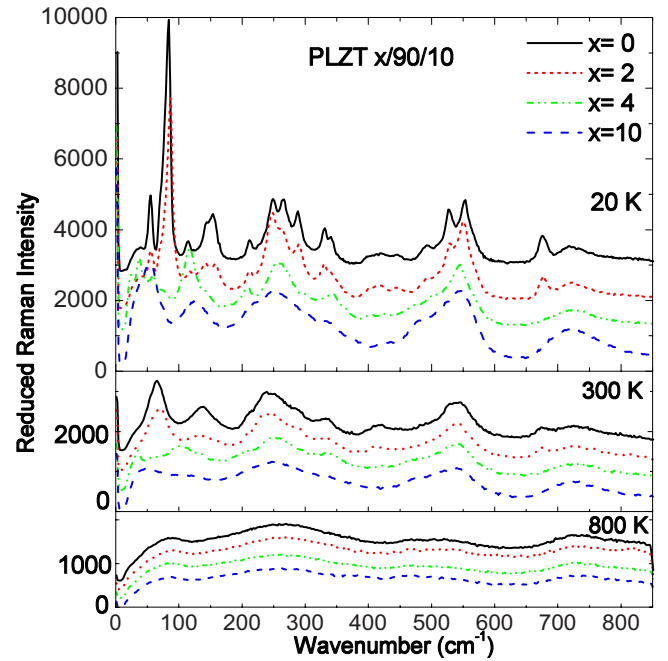


FIG. 3. (Color online) Raman spectra of PLZT  $X/90/10$  at different temperatures. At each temperature, spectra are vertically shifted for better visualization.

hertz range together with the calculated ones from the IR fit, are shown. Peaks that change their frequency and intensity with temperature are seen in all the samples, corresponding to excitations driving the phase transitions.

Raman spectra of the PLZT  $X/90/10$  samples are presented in Fig. 3 for selected temperatures. At high temperatures all the samples are in the cubic phase, and show a weak signal (as common in cubic perovskites). On cooling, samples with  $X=0, 2$  enter into the FE phase and samples with  $X=4, 10$  into the AFE one. At 300 K, samples  $X=0, 2$  have doubled rhombohedral cells. Their spectra show common features which are absent in the samples with  $X=4, 10$  (e.g., peaks at 140 and 680  $\text{cm}^{-1}$ ), confirming the change of symmetry between  $X=2$  and 4. At 20 K, these differences are even more pronounced.

The Raman and IR data on PLZT  $X/90/10$  reveal striking phonon-frequency anomalies in all the studied compositions (low-energy phonons are shown in Fig. 4). The most remarkable changes occur near the phase transition temperatures marked by vertical dotted lines. As La induces AFE state,<sup>6</sup> PLZT 4,10/90/10 are already macroscopically AFE (Ref. 7) although FE nanoclusters could be still present. The lowest-frequency mode (clearly seen in the terahertz spectra) corresponds to the FE (or AFE) soft mode in the samples. We fit its temperature dependence in the low temperature polar phase with the formula  $\omega^2 = a(T - T_C)^\gamma$ ; results of the fits are shown in Fig. 4 by solid lines. Rhombohedral FE samples ( $X=0, 2$ ) follow the classical Landau behavior and the Co-

TABLE I. Temperatures of the FE phase transitions in PLZT  $X/90/10$  samples.

% La	0	2	4	10
$T_C$	520	470	460	380
$T_{C'}$	360	365		

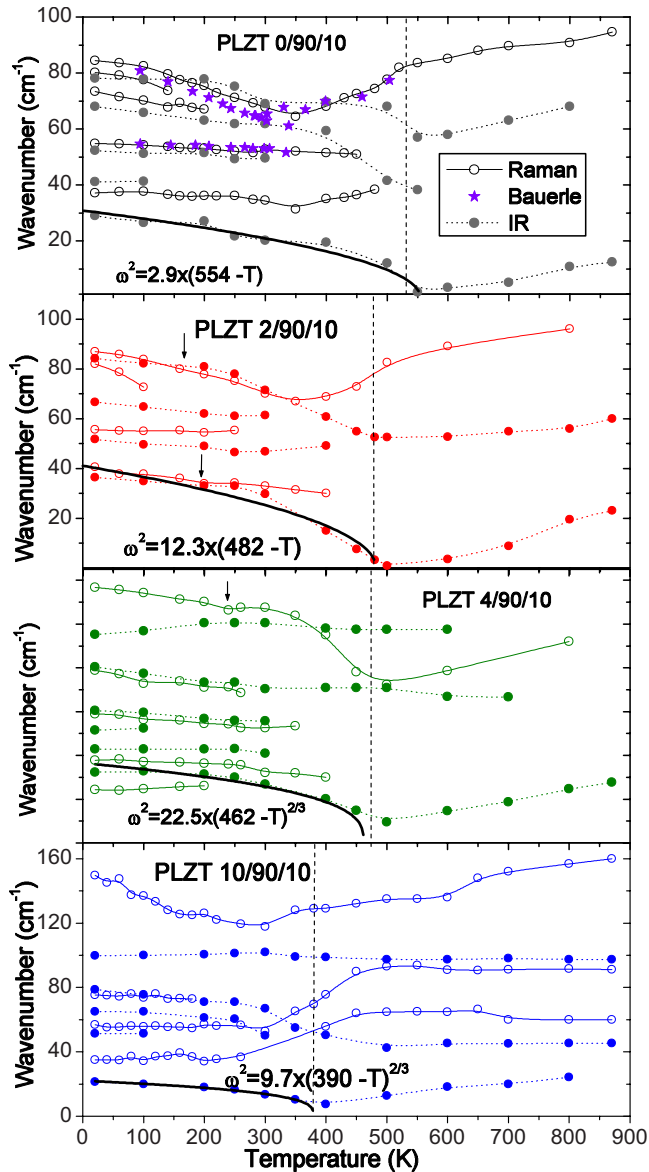


FIG. 4. (Color online) Temperature dependence of the low-frequency phonons in PLZT  $X/90/10$ . For  $X=0$  stars are frequencies by Bauerle (Ref. 8).

chran law with  $\gamma=1$ .<sup>15</sup> Tetragonal AFE samples ( $X=4, 10$ ) deviate from this behavior ( $\gamma=2/3$ ), probably due to the vicinity of a tricritical point (where PE, FE, and AFE states coexist).<sup>6</sup> The extrapolated  $T_C$  temperatures are in good agreement with the values in Table I.

Both rhombohedral samples show another IR active temperature dependent mode at higher frequencies (60–80  $\text{cm}^{-1}$ ), which seems to be coupled with the soft mode. However, anomalies in the Raman modes ( $X=0, 2$ ) occur also  $\sim 200$  K, below  $T_C$ . Note that the same minimum in the mode eigenfrequency was observed also by Bauerle *et al.*,<sup>8,9</sup> in PZT 90/10 [see Fig. 4(a)]. As these samples show a second phase transition connected with octahedra tilting, Raman anomalies could be related to them. Tetragonal AFE samples behave differently. PLZT 4/90/10 displays softening

of both IR and Raman active soft modes toward  $T_C$ , (see Fig. 4)—the second phase transition seems to be inhibited by the presence of La. The behavior of PLZT 10/90/10 is even more complex, probably due to coexistence phases,<sup>6,7</sup> and the phonon anomalies must be studied more in detail.

A closer look into Fig. 4 shows tiny anomalies near 200 K of two IR modes in PLZT 2/90/10 and of one Raman mode in PLZT 4/90/10 (marked by arrows in Fig. 4). Coexistence of FE, AFE, and incommensurate states in PLZT was revealed by the distribution of domains measured by TEM.<sup>16</sup> The theoretical studies by Ishchuk *et al.*<sup>6</sup> also explain the morphotropic phase boundary between the FE and the AFE phases in PLZT by the presence of AFE (or FE) clusters in a FE (or AFE) matrix depending on the amount of La. Whether these anomalies are due to phase transitions in nanoclusters should be further investigated.

We conclude that a change in symmetry in PLZT  $X/90/10$  between  $X=2$  and 4 is confirmed by our results. The phonon anomalies observed near  $T_C$  in IR spectra of all ceramics show that the FE/AFE phase transitions are driven by polar soft modes. A second phase transition connected with the doubling of the unit cell was detected by Raman in rhombohedral samples ( $X \leq 2$ ). The occurrence of further phonon anomalies at different temperatures speaks in favor of coexisting phases. The FE and AFE states could develop locally in different temperature ranges. In the tetragonal samples the polar soft modes do not obey the classical softening due to tricritical behavior induced by higher La concentration.

This work was supported by ASCR (Project Nos. IAA100100701, AVOZ10100520, KAN301370701), and GAČR (202/06/0403).

<sup>1</sup>C. E. Land, P. Thatcher, and G. H. Haertling, in *Advances in Materials and Device Research*, edited by R. Wolfe (Academic, New York, 1974), Vol. 4, pp. 137–233.

<sup>2</sup>H. Jaffe and D. A. Berlincourt, *Proc. IEEE* **53**, 1372 (1965).

<sup>3</sup>C. Michel, J. M. Moreau, G. D. Achenbach, R. Gerson, and W. J. James, *Solid State Commun.* **7**, 865 (1969).

<sup>4</sup>A. M. Glazer and S. A. Mabud, *Acta Crystallogr. B* **34**, 1060 (1978).

<sup>5</sup>E. Breval, C. Wang, and J. Dougherty, *J. Am. Ceram. Soc.* **88**, 437 (2005).

<sup>6</sup>V. M. Ishchuk, V. N. Baumer, and V. L. Sobolev, *J. Phys.: Condens. Matter* **17**, L177 (2005) (and references therein).

<sup>7</sup>J. Knudsen, D. I. Woodward, and I. M. Reaney, *J. Mater. Res.* **18**, 262 (2003).

<sup>8</sup>D. Bauerle and A. Pinczuk, *Solid State Commun.* **19**, 1169 (1976).

<sup>9</sup>D. Bauerle, R. Clarke, and T. P. Martin, *Phys. Status Solidi B* **71**, K173 (1975).

<sup>10</sup>S. Kamba, J. Peltzelt, J. Banys, R. Mizaras, J. Grigas, J. Pokorny, J. Endal, A. Brilingas, G. Komandin, A. Pronin, and M. Kosec, *Ferroelectrics* **223**, 247 (1999).

<sup>11</sup>T. Ostapchuk, V. Železný, and J. Peltzelt, *Proc. SPIE* **37**, 151 (1999).

<sup>12</sup>E. Buixaderas, I. Gregora, S. Kamba, J. Peltzelt, and M. Kosec, *J. Phys.: Condens. Matter* **20**, 345229 (2008).

<sup>13</sup>E. Buixaderas, D. Nuzhnyy, S. Veljko, M. Savinov, P. Vaněc, S. Kamba, J. Peltzelt, and M. Kosec, *Phase Transitions* **79**, 415 (2006).

<sup>14</sup>F. Gervais, in *Infrared and Millimeter Waves*, edited by K. J. Button (Academic, New York, 1983), Vol. 8, Chap. 7, p. 279.

<sup>15</sup>W. Cochran, *Phys. Rev. Lett.* **3**, 412 (1959).

<sup>16</sup>D. Viehland, X. H. Dai, J. F. Li, and Z. Xu, *J. Appl. Phys.* **84**, 458 (1998).